AMERICAN SOCIETY FOR MICROBIOLOGY | Applied and Environmental Microbiology®

BIODEGRADATION

Physiological Role of the Previously Unexplained Benzenetriol Dioxygenase Homolog in the *Burkholderia* sp. Strain SJ98 4-Nitrophenol Catabolism Pathway

Juan Liu,[a] Ying Xu,[a] Shi-Kai Deng,[a] Lei Liu,[a] Jun Min,[b] Ting Shi,[a] Jim C. Spain,[c] Ning-Yi Zhou[a]

[a]State Key Laboratory of Microbial Metabolism, Joint International Research Laboratory of Metabolic & Developmental Sciences and School of Life Sciences & Biotechnology, Shanghai Jiao Tong University, Shanghai, China

[b]Key Laboratory of Coastal Biology and Bioresource Utilization, Yantai Institute of Coastal Zone Research, Chinese Academy of Sciences, Yantai, Shandong, China

[c]Center for Environmental Diagnostics and Bioremediation, University of West Florida, Pensacola, Florida, USA

ABSTRACT 4-Nitrophenol, a priority pollutant, is degraded by Gram-positive and Gram-negative bacteria via 1,2,4-benzenetriol (BT) and hydroquinone (HQ), respectively. All enzymes involved in the two pathways have been functionally identified. So far, all Gram-negative 4-nitrophenol utilizers are from the genera *Pseudomonas* and *Burkholderia*. But it remains a mystery why *pnpG*, an apparently superfluous BT 1,2-dioxygenase-encoding gene, always coexists in the catabolic cluster (*pnpABCDEF*) encoding 4-nitrophenol degradation via HQ. Here, the physiological role of *pnpG* in *Burkholderia* sp. strain SJ98 was investigated. Deletion and complementation experiments established that *pnpG* is essential for strain SJ98 growing on 4-nitrocatechol rather than 4-nitrophenol. During 4-nitrophenol degradation by strain SJ98 and its two variants (*pnpG* deletion and complementation strains), 1,4-benzoquinone and HQ were detected, but neither 4-nitrocatechol nor BT was observed. When the above-mentioned three strains (the wild type and complementation strains with 2,2′-dipyridyl) were incubated with 4-nitrocatechol, BT was the only intermediate detected. The results established the physiological role of *pnpG* that encodes BT degradation *in vivo*. Biotransformation analyses showed that the *pnpA*-deleted strain was unable to degrade both 4-nitrophenol and 4-nitrocatechol. Thus, the previously characterized 4-nitrophenol monooxygenase $PnpA_{SJ98}$ is also essential for the conversion of 4-nitrocatechol to BT. Among 775 available complete genomes for *Pseudomonas* and *Burkholderia*, as many as 89 genomes were found to contain the putative *pnpBCDEFG* genes. The paucity of *pnpA* (3 in 775 genomes) implies that the extension of BT and HQ pathways enabling the degradation of 4-nitrophenol and 4-nitrocatechol is rarer, more recent, and likely due to the release of xenobiotic nitroaromatic compounds.

IMPORTANCE An apparently superfluous gene (*pnpG*) encoding BT 1,2-dioxygenase is always found in the catabolic clusters involved in 4-nitrophenol degradation via HQ by Gram-negative bacteria. Our experiments reveal that *pnpG* is not essential for 4-nitrophenol degradation in *Burkholderia* sp. strain SJ98 but instead enables its degradation of 4-nitrocatechol via BT. The presence of *pnpG* genes broadens the range of growth substrates to include 4-nitrocatechol or BT, intermediates from the microbial degradation of many aromatic compounds in natural ecosystems. In addition, the existence of *pnpCDEFG* in 11.6% of the above-mentioned two genera suggests that the ability to degrade BT and HQ simultaneously is ancient. The extension of BT and HQ pathways including 4-nitrophenol degradation seems to be an adaptive evolution for responding to synthetic nitroaromatic compounds entering the environment since the industrial revolution.

KEYWORDS 4-nitrophenol, 4-nitrocatechol, 1,2,4-benzenetriol 1,2-dioxygenase, *Burkholderia* sp. strain SJ98

Citation Liu J, Xu Y, Deng S-K, Liu L, Min J, Shi T, Spain JC, Zhou N-Y. 2021. Physiological role of the previously unexplained benzenetriol dioxygenase homolog in the *Burkholderia* sp. strain SJ98 4-nitrophenol catabolism pathway. Appl Environ Microbiol 87:e00007-21. https://doi.org/10.1128/AEM.00007-21.

Editor Shuang-Jiang Liu, Chinese Academy of Sciences

Address correspondence to Ying Xu, ying.xu@sjtu.edu.cn.

Received 8 January 2021
Accepted 6 May 2021
Accepted manuscript posted online 14 May 2021
Published 25 June 2021

Nitrophenols, widely used in agriculture and industry, are toxic and widely distributed in the environment (1, 2). A variety of bacteria have been isolated for their ability to degrade 4-nitrophenol (PNP) (3–9).

To date, two distinct catabolic pathways for PNP degradation have been elucidated in detail. In Gram-positive bacteria such as *Bacillus sphaericus* JS905 (8), *Rhodococcus opacus* SAO101 (9), and *Arthrobacter* sp. strain JS443 (10, 11), PNP is degraded via the 1,2,4-benzenetriol (BT) pathway, in which BT 1,2-dioxygenase catalyzes ring cleavage (Fig. 1). In this pathway, PNP is sequentially transformed into 4-nitrocatechol (4-NC) and BT in turn by a two-component PNP monooxygenase such as NpcAB (accession numbers BAD30042 and BAD30041) from strain SAO101 (9) and NpdA1A2 (accession numbers ABL75140 and ABL75143) from strain JS443 (10). BT then undergoes ring cleavage before entering the central metabolism. The BT 1,2-dioxygenases $NpcC_{SAO101}$ (accession number BAD30043) from strain SAO101 (9) and $NpdB_{JS443}$ (accession number ABL75139) from strain JS443 (10) were both functionally identified as catalyzing the ring cleavage reaction of BT. In contrast, PNP is degraded via the hydroquinone (HQ) pathway by Gram-negative strains such as *Pseudomonas* sp. (formerly *Moraxella* sp.) strain JS425 (6, 12), *Pseudomonas* sp. strain WBC-3 (5), *Pseudomonas putida* DLL-E4 (3), *Burkholderia* sp. strain SJ98 (13), *Pseudomonas* sp. strain 1-7 (7), and *Pseudomonas* sp. strain NyZ402 (4). To date, all known Gram-negative PNP degraders are from two common genera, *Pseudomonas* and *Burkholderia* (3–7, 13). In strains SJ98, WBC-3, DLL-E4, NyZ402, and 1-7, it is clearly established that PNP is catabolized via HQ as the ring cleavage intermediate, and the complete degradation was catalyzed by PnpABCDEF (3–5, 14) or their homologous enzymes (3, 5, 7), without the involvement of PnpG or its homologs (Fig. 1).

Interestingly, among the *pnp* and *pnp*-like clusters from the identified Gram-negative PNP utilizers, a *pnpG*-encoded BT 1,2-dioxygenase homolog always coexists with the other *pnp* genes involved in PNP degradation via HQ (Fig. 1). There is no obvious role for PnpG and its homologous enzymes during PNP degradation via HQ as shown in the top panel (for Gram-negative strains) of Fig. 1l (3–5, 7). Strain SJ98, a representative of Gram-negative PNP utilizers, has a catabolic cluster containing *pnpABCDEFG* (13) (Fig. 1). $PnpA_{SJ98}$ and $PnpB_{SJ98}$ are a single-component PNP 4-monooxygenase and a 1,4-benzoquinone (BQ) reductase, respectively (14). PnpCDEF from strain SJ98 catalyze HQ ring cleavage and subsequent reactions leading to the central metabolism (13). $PnpG_{SJ98}$ (accession number EKS70669) and its homologs from Gram-negative PNP utilizers showed moderate identities (about 40%) with the identified BT 1,2-dioxygenases $NpcC_{SAO101}$ and $NpdB_{JS443}$ from Gram-positive bacteria capable of PNP degradation via BT. Although $PnpG_{SJ98}$ catalyzes the ring cleavage of BT *in vitro* (15) like the BT 1,2-dioxygenase $PnpG_{WBC-3}$ from strain WBC-3 (16), and BT 1,2-dioxygenase activity was detected *in vivo* during PNP degradation by *Pseudomonas* sp. strain JS425 (6), the physiological role of $PnpG_{SJ98}$ and its homologs *in vivo* is unknown.

Here, we establish the physiological role of $PnpG_{SJ98}$ *in vivo* and the inducer for the transcription of the *pnpA* and *pnpG* genes from strain SJ98. Furthermore, we also analyzed the frequency of the coexistence of *pnpG* and its homologs with the putative PNP catabolic genes in the reported genomes from two common genera of Gram-negative PNP utilizers. The findings solve the long-standing mystery that the apparently superfluous gene (*pnpG*) always coexists in the catabolic cluster (*pnpABCDEF*) encoding PNP degradation via HQ in Gram-negative utilizers.

RESULTS

***pnpG* is not essential for PNP degradation by strain SJ98.** To explore the physiological function of *pnpG in vivo*, strains SJ98, SJ98Δ*pnpG*, and SJ98Δ*pnpG*(pRK415-*pnpG*) were grown with PNP in minimal medium (MM), and the negative controls were three strains in MM without PNP. Strain SJ98 and its two variants were all able to utilize PNP for growth (Fig. 2). In particular, the deletion of *pnpG* had no effect on the growth of strain SJ98Δ*pnpG* with PNP as the sole carbon source (Fig. 2b). To better illustrate their growth with PNP, these three strains were incubated with a low initial optical density at 600 nm (OD_{600}) value. They all grew, whereas negative controls did not

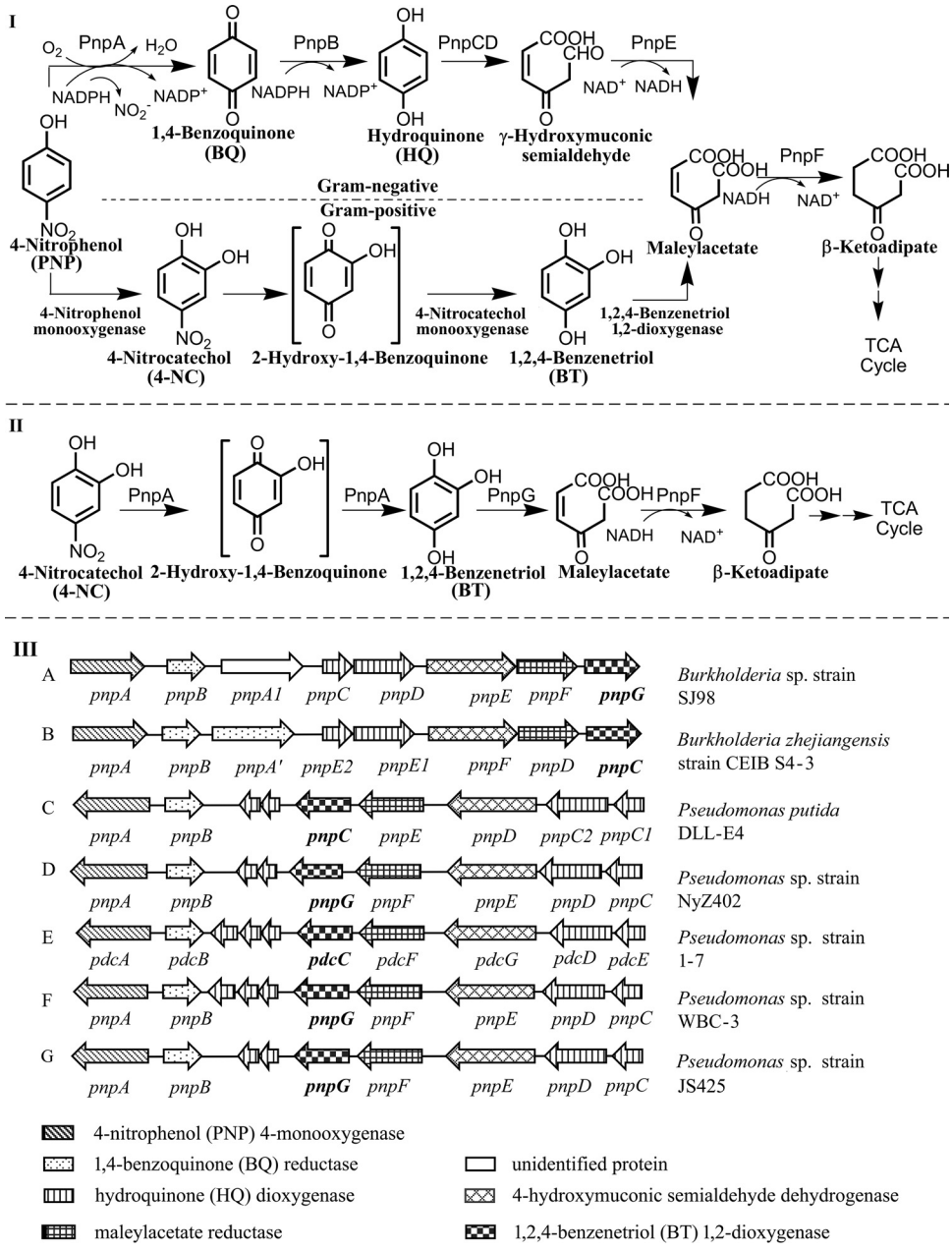

FIG 1 (I) Catabolic pathways for PNP degradation in Gram-positive and Gram-negative strains. (II) Proposed pathway of 4-NC degradation in strain SJ98. (III) Comparison of the genetic organizations of PNP catabolic clusters from different PNP utilizers. (A) The PNP catabolic cluster in *Burkholderia* sp. strain SJ98 (14, 41); (B) the PNP catabolic cluster in *Burkholderia zhejiangensis* strain CEIB S4-3 (42); (C) the PNP catabolic cluster in *Pseudomonas putida* DLL-E4 (3); (D) the PNP catabolic cluster in *Pseudomonas* sp. strain NyZ402 (4); (E) the PNP catabolic cluster in *Pseudomonas* sp. strain 1-7 (7); (F) the PNP catabolic cluster in *Pseudomonas* sp. strain WBC-3 (5); (G) the PNP catabolic cluster in *Pseudomonas* sp. strain JS425. The GenBank accession numbers of all the above-mentioned PNP catabolic gene clusters are shown in Table S1 in the supplemental material. TCA, tricarboxylic acid.

(see Fig. S1a in the supplemental material), which were similar to those shown in Fig. 2. The intermediates BQ and HQ accumulated transiently during PNP degradation by all three strains (Fig. 2). The results established that *pnpG* was not essential for PNP degradation via HQ by strain SJ98.

Neither 4-NC nor BT was detected during PNP degradation by strain SJ98 and its two variants. These results were different from a previous report in which both 4-NC and BT were detected during PNP degradation in this strain (17).

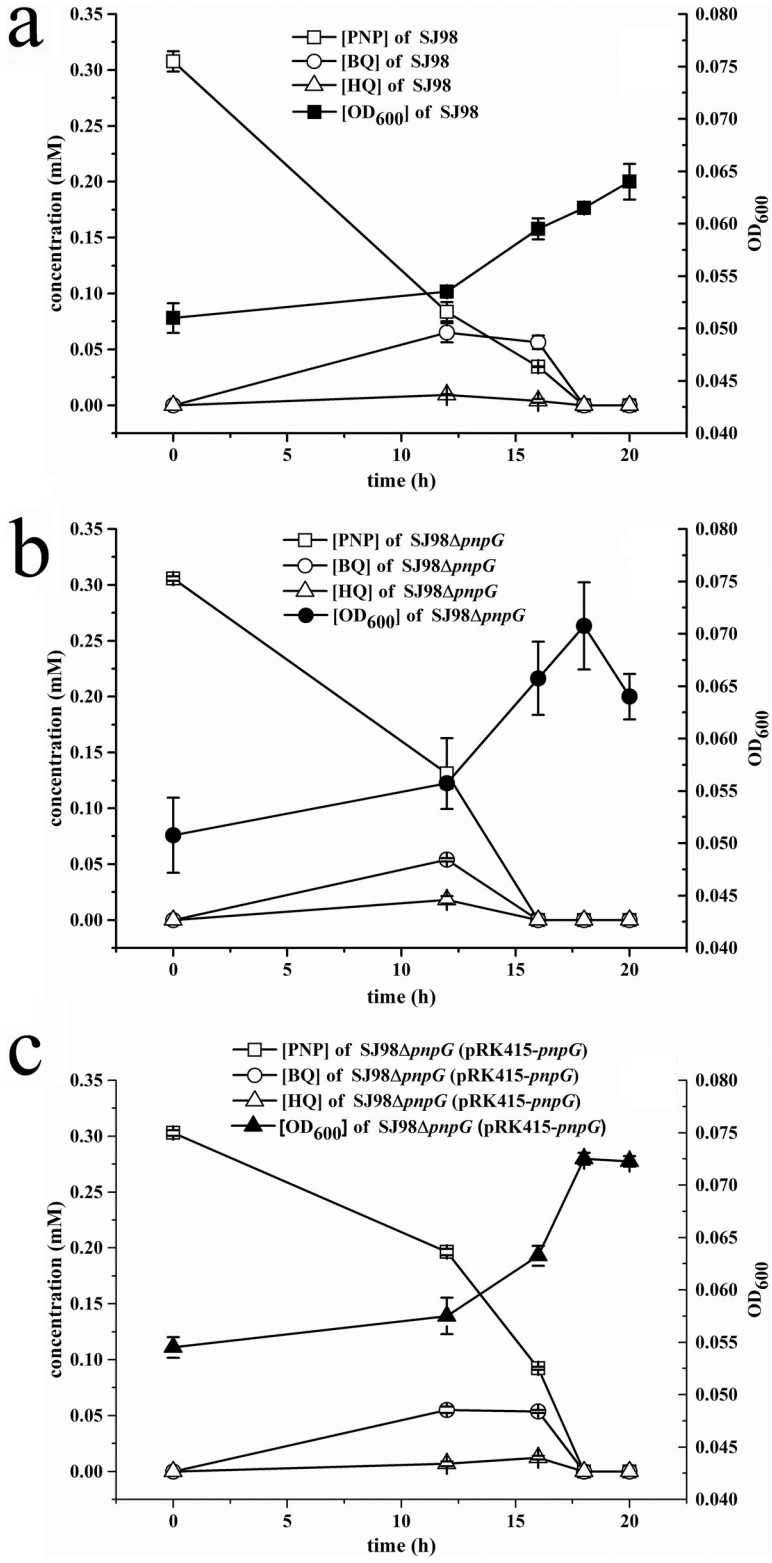

FIG 2 Time course assay of PNP degradation and the growth of *Burkholderia* sp. strain SJ98 and its derivatives. Strains were grown in MM with 0.3 mM PNP as the sole carbon source at 30°C. The consumption of PNP and the accumulation of BQ and HQ during the growth of strains SJ98 (a), SJ98Δ*pnpG* (with *pnpG* deleted) (b), and SJ98Δ*pnpG*(pRK415-*pnpG*) (c) were quantified by HPLC. The symbols indicate the means for three replicates, and error bars indicate standard deviations of the means ($n = 3$).

***pnpG* is crucial for the growth of strain SJ98 on 4-NC.** To further explore the physiological function of *pnpG in vivo*, strain SJ98 and its two variants were grown with 4-NC (the substrate of the PnpG-like enzyme in Gram-positive strains) in MM, and the negative controls were these three strains in MM without 4-NC. Strain SJ98 was able to utilize 4-NC for its growth, but the mutant strain SJ98Δ*pnpG* completely lost this ability. With the complementation of *pnpG*, the ability was restored in strain SJ98Δ*pnpG* (pRK415-*pnpG*) (Fig. 3a). To better illustrate their growth with 4-NC, these three strains were incubated at a low initial OD_{600} value. The wild-type and complementation strains grew, whereas the mutant strain and negative controls did not (Fig. S1b), which were similar to those shown in Fig. 3a. All the results indicated that *pnpG* was necessary for the growth of strain SJ98 on 4-NC. Meanwhile, as shown in Fig. 3b, 4-NC was completely consumed by strain SJ98 and its two variants after 11 h, but only the mutant strain accumulated the dead-end intermediate BT due to the absence of *pnpG*. The lack of stoichiometry between 4-NC consumption and BT accumulation was probably due to the auto-oxidation of BT (8). These results established the physiological role of *pnpG* during the growth of strain SJ98 on 4-NC.

$PnpG_{SJ98}$ catalyzes the oxidation of BT converted from 4-NC *in vivo*. To capture the intermediates and identify the oxidation of BT catalyzed by $PnpG_{SJ98}$ during 4-NC degradation, biotransformation experiments were performed with resting cells of strain SJ98 and its two variants. As shown in Fig. 4, 4-NC was consumed similarly by strain SJ98 and its two variants. Additionally, when the activity of nonheme iron-dependent aromatic ring dioxygenases in strains SJ98 and SJ98Δ*pnpG*(pRK415-*pnpG*) was inhibited by 2,2′-dipyridyl, both could accumulate BT exactly like the mutant strain SJ98Δ*pnpG* (Fig. 4). During the consumption of 4-NC, BT accumulated and then decreased slightly (Fig. 4), probably due to the auto-oxidation of BT (8). No other intermediates were detected during the biotransformation. This indicated that $PnpG_{SJ98}$ catalyzes the oxidation of BT from 4-NC *in vivo*, analogous to the function of its homologs in Gram-positive PNP utilizers (Fig. 1).

$PnpA_{SJ98}$ catalyzed the oxidation of 4-NC to BT. In addition to $PnpA_{SJ98}$ catalyzing the oxidation of PNP to form BQ rather than 4-NC, it catalyzes the transformation of 4-NC (13, 14). To explore whether $PnpA_{SJ98}$ is involved in the first step of 4-NC conversion to BT, biotransformation of 4-NC was performed. Resting cells of *Escherichia coli* strain BL21(pGEX-6P-1-*pnpA*) converted 4-NC to BT, whereas strain BL21 did not (Fig. 5). Consistent with the presumed auto-oxidation of BT (8), 4-NC conversion to BT was not stoichiometric. The results established the role of $PnpA_{SJ98}$ in catalyzing the oxidation of 4-NC to BT (Fig. 1). Therefore, strain SJ98 expressed the complete pathway for 4-NC degradation. In contrast, cells of SJ98Δ*pnpA* were not able to degrade PNP or 4-NC (Fig. S2), suggesting that no additional monooxygenases in strain SJ98 catalyze the conversion of PNP to 4-NC or 4-NC to BT.

Both PNP and 4-NC induced the enzymes of the 4-NC degradation pathway. To investigate the regulation of 4-NC degradation in strain SJ98, transcriptional analyses of *pnpA* and *pnpG* under various induction conditions were conducted by real-time quantitative PCR (RT-qPCR). The relative transcription levels of *pnpA* and *pnpG* after induction with 4-NC were 49.6- and 6.4-fold higher than those in uninduced controls, which means that 4-NC upregulates the genes encoding enzymes for the degradation of 4-NC (Fig. 6). In addition, PNP stimulated 38.6- and 5.1-fold upregulations of *pnpA* and *pnpG* (Fig. 6). The results of RT-qPCR indicated that both PNP and 4-NC served as efficient inducers of 4-NC degradation. Given that all *pnp* genes from strain SJ98 were in a single operon (13), 4-NC seemed to be able to induce the transcription of the complete *pnp* gene cluster involved in PNP and 4-NC degradation, which has not been reported previously.

Genome sequencing and reclassification of strain JS425. Strain JS425, initially identified as a member of the *Moraxella* genus, was the first functionally identified PNP utilizer (6, 12). However, the PNP catabolic cluster or the genome sequence of strain JS425 was not reported. Therefore, we sequenced the genome. The complete 16S rRNA gene from this strain exhibited the highest identity (>99%) to the 16S rRNA genes from three strains of the genus *Pseudomonas* (accession numbers DQ453810, DQ785814,

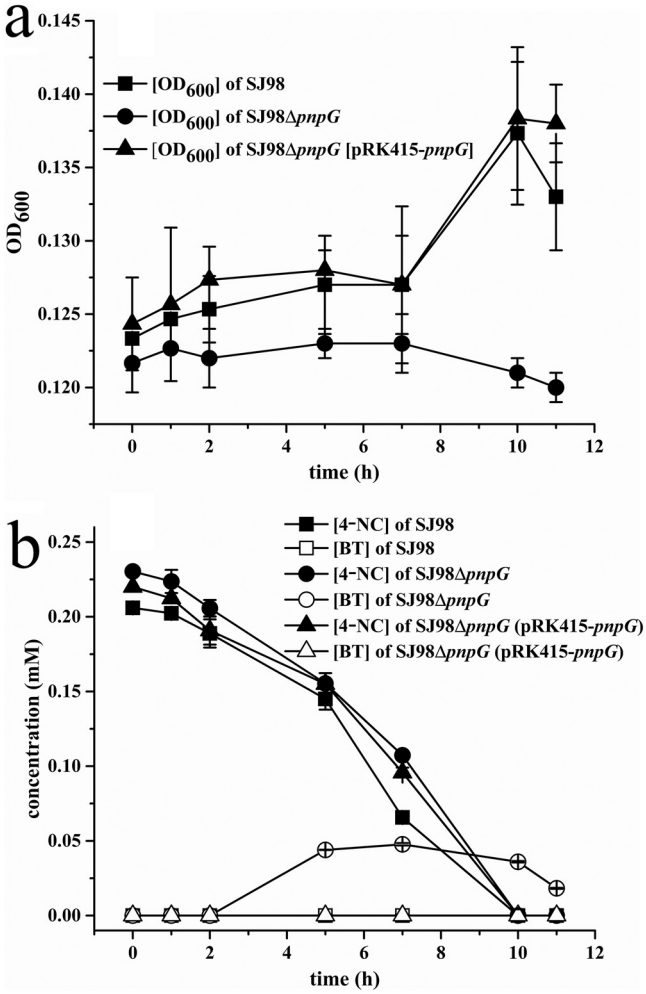

FIG 3 Time course assay of 4-NC degradation and the growth of *Burkholderia* sp. strain SJ98 and its derivatives. Strains were grown in MM with 0.2 mM 4-NC as the sole carbon source at 30°C. (a) Growth curves of strain SJ98 and its derivatives on 4-NC. (b) The consumption of 4-NC and the accumulation of BT were quantified by HPLC. The symbols indicate the means for three replicates, and error bars indicate standard deviations of the means ($n = 3$).

and FR682933), indicating that it should be reclassified as a *Pseudomonas* sp. rather than as a *Moraxella* sp. as originally classified (6, 12).

Bioinformatic evidence indicating the coexistence of *pnpG* and its homologs with catabolic clusters encoding PNP degradation via HQ from *Pseudomonas* spp. and *Burkholderia* spp. To date, all identified Gram-negative PNP utilizers fall into the genera *Burkholderia* and *Pseudomonas*. In total, 775 complete genomes from *Burkholderia* spp. (259 genomes) and *Pseudomonas* spp. (516 genomes) were obtained from the NCBI complete genome database (Table S2). All annotated proteins from the 775 complete genomes showed no more than 30% identities with $PnpA_{SJ98}$ except for PnpA from *Pseudomonas putida* DLL-E4 (accession number CP007620) (77% identity), PnpA from *Pseudomonas* sp. strain JS425 (accession number CP073661) (76% identity), and PnpA from *Burkholderia* sp. strain YI23 (accession number CP003087) (96% identity).

Among the 775 Gram-negative genomes, the complete PNP cluster *pnpABCDEFG* is retrieved only from genomes of strains DLL-E4, YI23, and JS425, with each protein exhibiting ≥40% identities with their counterparts in PnpABCDEFG from strain SJ98 (Fig. 7). If *pnpA* is omitted, however, genes encoding PnpBCDEFG exist in as many as 59 genomes from *Burkholderia* and 30 genomes from *Pseudomonas* (Fig. 7). In addition to strain YI23, 58 genomes from *Burkholderia* possessed genes encoding proteins

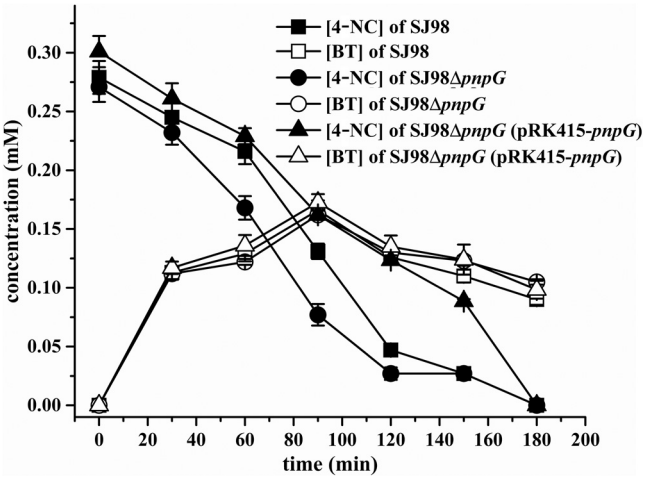

FIG 4 Biotransformation of 4-NC by resting cells of *Burkholderia* sp. strain SJ98 and its derivatives. Biotransformation was initiated by adding 0.3 mM 4-NC. At appropriate intervals, 0.5-ml samples were withdrawn from the system, mixed with an equal volume of methanol, and shaken vigorously for 5 min to stop the reaction. After centrifugation, the supernatants of samples were used to analyze the disappearance of the substrate (4-NC) and the appearance of the products (BT) by HPLC. Quantitative analysis was performed using a standard curve of authentic standards. The symbols indicate the means for three replicates, and error bars indicate standard deviations of the means ($n = 3$).

exhibiting 25% to 30% identities with $PnpA_{SJ98}$, and 16 out of 30 genomes from *Pseudomonas* possessed genes encoding proteins exhibiting 23% to 30% identities with $PnpA_{SJ98}$. Moreover, all of the above-mentioned putative enzymes are annotated as flavin adenine dinucleotide (FAD)-dependent oxidoreductases, and some of the encoding genes are clustered with or in the vicinity of *pnpBCDEF*. But due to their low identities with $PnpA_{SJ98}$, they cannot be certainly considered PnpA homologs. If both *pnpA* and *pnpB*, the two genes encoding the conversion of PNP to HQ, are omitted, cluster *pnpCDEFG* is present in 90 genomes (11.6% of 775 genomes), 60 from *Burkholderia* and 30 from *Pseudomonas* (Fig. 7). Interestingly, cluster *pnpCDEF* without *pnpG* is found in only 3 genomes

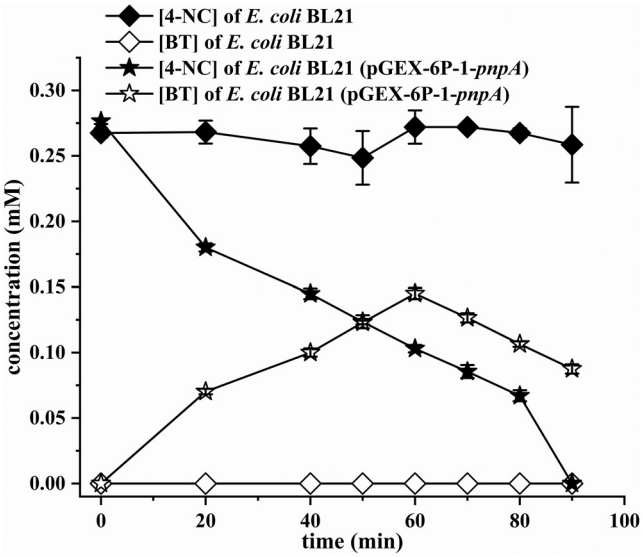

FIG 5 Biotransformation of 4-NC by resting cells of *E. coli* BL21(DE3)(pGEX-6P-1-*pnpA*). Biotransformation was initiated by adding 0.3 mM 4-NC. At appropriate intervals, 0.5-ml samples were withdrawn from the system, mixed with an equal volume of methanol, and shaken vigorously for 5 min to stop the reaction. After centrifugation, the supernatants of samples were used to analyze the disappearance of the substrate (4-NC) and the appearance of the products (BT) by HPLC. The symbols indicate the means for three replicates, and error bars indicate standard deviations of the means ($n = 3$).

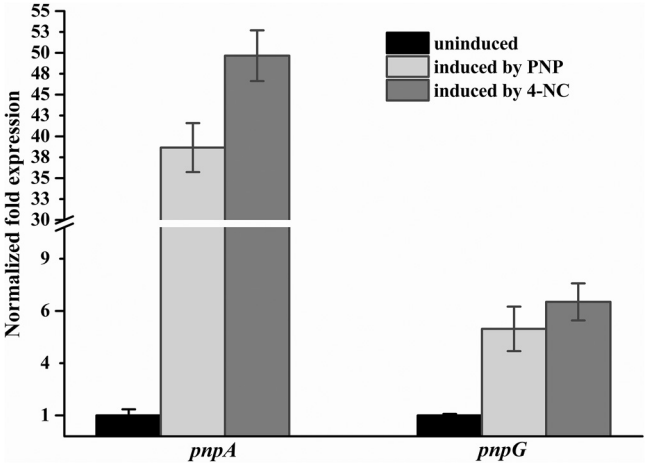

FIG 6 Transcriptional analysis of *pnpA* and *pnpG* in *Burkholderia* sp. strain SJ98 under induced and uninduced conditions by RT-qPCR. Strain SJ98 was grown in MM with 2 mM glucose to an OD_{600} of 0.3 and then induced with 0.1 mM 4-NC or 0.3 mM PNP for 5 h. Cells incubated without 4-NC or PNP induction were used as the negative control. The expression levels of each tested gene were calculated with the cycle threshold ($2^{-\Delta\Delta CT}$) method. The results are the averages from three independent measurements, and error bars indicate standard deviations of the means ($n = 3$).

(all in *Burkholderia*) (Fig. 7). Several clusters with partial *pnp* genes are also present. For instance, cluster *pnpEFG* is in 13 genomes (11 from *Burkholderia* and 2 from *Pseudomonas*), *pnpBFG* is in 2 genomes (*Pseudomonas*), *pnpBEF* is in 1 genome (*Burkholderia*), and *pnpEG* is in 1 genome (*Pseudomonas*).

It can be concluded that the BT 1,2-dioxygenase-encoding gene *pnpG* is always clustered with the putative cluster *pnpCDEF* for HQ degradation, but *pnpA* (3 of 775 genomes) is quite rare.

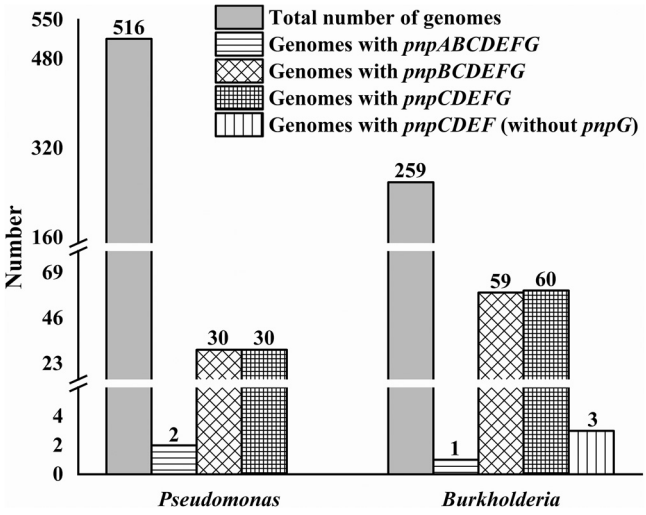

FIG 7 Abundance of the *pnp* cluster in the genomes from the genera *Pseudomonas* and *Burkholderia*. Among the protein sequences encoded by 775 bacterial genomes from *Pseudomonas* and *Burkholderia*, those from *Pseudomonas* sp. strain JS425 were sequenced and annotated in this study, and the others were downloaded from the Complete Microbial Genomes Database of the National Center for Biotechnology Information (NCBI) in May 2020. All of them were used to build a local BLAST database. BLASTp searches were performed with PnpA, PnpB, PnpC, PnpD, PnpE, PnpF, and PnpG against these 775 completely sequenced bacterial genomes. Total number of genomes, the number of genomes obtained from *Burkholderia* and *Pseudomonas* with complete genome sequences from the NCBI; Genomes with *pnpABCDEFG*, the number of genomes possessing putative PnpABCDEFG-encoding genes; Genomes with *pnpBCDEFG*, the number of genomes possessing putative PnpBCDEFG-encoding genes; Genomes with *pnpCDEFG*, the number of genomes possessing putative PnpCDEFG-encoding genes; Genomes with *pnpCDEF* (without *pnpG*), the number of genomes possessing putative PnpCDEF-encoding genes but without PnpG-encoding genes.

DISCUSSION

pnpG and its homologs from identified and putative Gram-negative PNP utilizers are linked to catabolic genes involved in PNP degradation via HQ (Fig. 1). In strain SJ98, $PnpG_{SJ98}$ was established as a BT 1,2-dioxygenase essential for 4-NC rather than PNP degradation *in vivo*. PNP was degraded only via HQ, which is different from previous observations that PNP was degraded via 4-NC and BT (15, 17). $PnpA_{SJ98}$ catalyzed the reaction of not only PNP to BQ but also 4-NC to BT, which was similar to those of the other two strains, DLL-E4 and WBC-3 (3, 16). No additional monooxygenases in strain SJ98 nonspecifically converted PNP to 4-NC (see Fig. S2 in the supplemental material). The presence of *pnpG* and its homologs conferred on strain SJ98 and the other two strains the ability to mineralize 4-NC in addition to PNP. Indeed, it was reported that many nitroaromatic compounds such as PNP, 4-NC, methylnitrophenols, and dinitrophenol (DNP) were simultaneously detected in particles associated with biomass burning (18, 19). Thus, the presence of *pnpG* and its homologs may provide a selective advantage to strain SJ98 and other Gram-negative PNP utilizers in environments contaminated with mixtures of nitrophenols.

BT is an environmental pollutant (20) and is commonly used in hair dyes (21). It is also an intermediate or a metabolite during the microbial degradation of several aromatic compounds, including resorcinol, PNP, *meta*-nitrophenol (MNP), 4-NC, 2,4-dinitrophenol (2,4-DNP), 4-chlorophenol (4-CP), and 4-nitroanisole (Table 1). It is generally accepted that microbes exist in communities in nature where both xenobiotic pollutants and natural organic compounds are present in mixtures. Several strains possessing only subsets of pathway genes degraded aromatic compounds through the concerted actions of various cryptic pathways (22). Thus, the growth of a strain on a single compound as the sole carbon source is likely to be the exception in natural habitats. Therefore, for strain SJ98 and other Gram-negative PNP utilizers living in microbial communities, the presence of *pnpG* and its homologs probably conferred the additional ability to utilize BT converted from aromatic compounds by other microbes (Table 1) in communities. They thus obtained more chances for survival in the environment contaminated with other aromatics in addition to PNP, 4-NC, and BT. This provides an example that an extra functional gene could offer the hosts more chances for survival in a contaminated environment.

Although two other Gram-negative PNP utilizers, strains DLL-E4 (3) and WBC-3 (5, 16), both possessed the genes for complete 4-NC degradation like strain SJ98, their PNP degradation was not induced by 4-NC, so they cannot degrade 4-NC alone without PNP as an inducer (3, 16). Unlike the two former strains, the *pnp* cluster was reported to be expressed in a single operon in strain SJ98 (13); both 4-NC and PNP induced the transcription of *pnp* genes in the present study. In contrast, due to the same gene arrangements and similar induced expression characteristics, the *pnp* genes from strain DLL-E4 (3) may also be located on three operons as reported for strain WBC-3 (16). $PnpG_{SJ98}$ and $PnpA_{SJ98}$ both showed about 50% and 80% identities with their homologs from strains DLL-E4 (3) and WBC-3 (16), respectively. Considering that they share catabolic enzymes but have different operon organizations, different Gram-negative PNP utilizers can be thought to have the same origin of *pnp* catabolic genes but organize them independently with different transcriptional regulation mechanisms.

As the cluster *pnpCDEFG* is present in as many as 11.6% (90/775) of the genomes in the two Gram-negative genera to which all PNP utilizers belong, it can be proposed that *pnpCDEFG* in most of these 90 genomes may well form a single operon, the same as in strain WBC-3 (16). Strains with this compact operon encoding four enzymes can potentially survive on either HQ or BT, which were intermediates from the microbial degradation of many aromatic compounds in the soil. During the evolution of the PNP degradation pathway, the Gram-negative strains containing only *pnpCDEFG* likely became PNP utilizers by recruiting *pnpAB* from other coexisting strains or by the evolution of FAD-dependent oxidoreductases with another catalytic function. Thus, although *pnpG* has no response to PNP degradation via HQ, the preexisting operon *pnpCDEFG* has naturally

TABLE 1 Different sources of BT in metabolic pathways[a]

Strain	Substrate	Metabolite(s)	Reference(s)
Arthrobacter sp. strain JS443	PNP	BT	11
Arthrobacter sp. strain Y1	PNP	BT	43
Burkholderia sp. strain Ku46	2,4-Dinitrophenol	PNP, BT	44
Pseudomonas sp. strain B2	MNP	BT	45
Serratia sp. strain DS001	PNP	BT	46
Rhodococcus sp. strain BPG-8	Resorcinol	BT	47, 48
Pseudomonas putida O1	Resorcinol	BT	49
Ochrobactrum sp. strain B2	4-NC	BT	50
Cupriavidus sp. strain CNP-8	2C4NP	BT	51
Arthrobacter chlorophenolicus A6	4-CP	BT	28
Rhodococcus opacus strain AS2	4-Nitroanisole	BT	31
Rhodococcus erythropolis strain AS3	4-Nitroanisole	BT	31

[a]PNP, 4-nitrophenol; BT, 1,2,4-benzenetriol; MNP, *meta*-nitrophenol; 4-NC, 4-nitrocatechol; 2C4NP, 2-chloro-4-nitrophenol; 4-CP, 4-chlorophenol.

led to the existence of *pnpG* in the catabolic clusters in Gram-negative PNP utilizers found in nature.

On the other hand, it is well known that many natural phenolic compounds are released from plants through leaching of aboveground parts, root exudation, and decomposition of plant residues (23–27). In general, soil bacteria are likely surrounded by phenols from the degradation of lignin (26); their ability to degrade BT and HQ should thus be ancient. The BT 1,2-dioxygenase might be a remnant from evolution, or it might be involved in mopping up trihydroxy aromatic compounds. The earliest pathways for HQ degradation might have involved hydroxylation to BT (28, 29). Any organism that recruited or evolved an enzyme for the direct cleavage of HQ would have a selective advantage because FAD monooxygenases are energetically expensive. The shunting of half of the reducing equivalents in the reaction from NADH to make water as a by-product means that those electrons cannot be used for ATP generation during oxidative phosphorylation. The elimination of one of the monooxygenase reactions by direct fission of the ring is a more direct route with minimal loss of reducing potential. With the development of industry and agriculture in the last 100 years, many aromatic xenobiotics also entered the environment. Bacterial degradation of halogenated aromatic compounds (28, 30), aminophenol (29), nitrophenols (8, 9), and methyl parathion (5) via BT and/or HQ pathways has been reported. Thus, the extension of the BT and/or HQ pathway for the degradation of these xenobiotics, including nitrophenols, would likely be rarer and more recent than the occurrence of BT and/or HQ pathways in nature. Many natural or xenobiotic nitroaromatic compounds, such as nitroanisole (31) and methyl parathion (5), are degraded via nitrophenol. It is tempting to speculate that the massive use of methyl parathion and similar pesticides stimulated the worldwide evolution or dispersion of nitrophenol catabolic pathways. The extension of BT and HQ pathways to include PNP degradation seems to be an adaptive evolution for responding to synthetic nitroaromatic compounds entering the environment as a result of human activities in the recent past.

The evolutionary trajectory of the PNP catabolic pathways is likely to remain speculative. It is clear from our results, however, that the current physiological role of *pnpG* in PNP catabolic clusters is to extend the capabilities of the system to include the degradation of 4-NC.

MATERIALS AND METHODS

Chemicals, strains, primers, media, and growth conditions. 4-Nitrophenol (PNP) (purity grade, ≥99%), 4-nitrocatechol (4-NC) (purity grade, ≥97%), 1,4-benzoquinone (BQ) (purity grade, ≥99.5%), hydroquinone (HQ) (purity grade, ≥99%), and 1,2,4-benzenetriol (BT) (purity grade, ≥99%) were all purchased from Sigma Chemical Company (St. Louis, MO, USA) or Fluka Chemical Company (Buchs, Switzerland). Restriction enzymes and the In-Fusion HD cloning kit were purchased from TaKaRa Biomedical Technology Co. Ltd. (Beijing, China). Plasmid DNA extraction and DNA gel extraction kits were purchased from Omega Bio-Tek Inc. (Doraville, GA). Strains and plasmids are listed in Table 2.

TABLE 2 Strains and plasmids used in this study

Strain or plasmid	Characteristic(s) and/or relevant genotype	Reference(s) or source
Strains		
Burkholderia sp. strain SJ98	PNP and 4-NC utilizer; wild type	52
Burkholderia sp. strain SJ98Δ*pnpG*	SJ98 mutant with the *pnpG* gene deleted	This study
Burkholderia sp. strain SJ98Δ*pnpG*(pRK415-*pnpG*)	*pnpG* gene complemented by pRK415-*pnpG* in SJ98Δ*pnpG*	This study
Burkholderia sp. strain SJ98Δ*pnpA*	SJ98 mutant with the *pnpA* gene deleted	13
E. coli DH5α	*supE44 lacU169* (φ80*lacZ*ΔM15) *recA1 endA1 hsdR17 thi-1 gyrA96 relA1*	Novagen
E. coli WM3064	Donor strain for conjugation; 2,6-diaminopimelic acid auxotroph; *thrB1004 pro thi rpsL hsdS lacZ*ΔM15 *RP4-1360* Δ(*araBAD*)*567* Δ*dapA1341*::(*erm pir* [wild type])	Novagen
E. coli BL21(DE3)	F^- *ompT hsdS*$_B$(r_B^- m_B^-) *gal* (λcI857 *ind1 sam7 nin5 lacUV5*-T7 gene 1) *dcm* (DE3)	Novagen
Plasmids		
pK18*mobsacB*	Widely used gene knockout vector; Km^r	35, 36
pK18*mobsacB-pnpG*	*pnpG* gene knockout vector containing 2 DNA fragments homologous to the upstream and downstream regions of *pnpG*	This study
pRK415	Broad-host-range vector; Tc^r	13, 38
pRK415-*pnpG*	Vector for *pnpG* gene complementation made by fusion of *pnpA* to pRK415 at PstI/KpnI restriction sites	This study
pGEX-6P-1	Km^r; source of the *tac* promoter	Amersham
pGEX-6P-1-*pnpA*	Plasmid for expression of *pnpA*	This study

Primers are listed in Table 3. *E. coli* strains were grown in lysogeny broth (LB) (32, 33) at 37°C. Strain SJ98 and its derivatives were grown in LB or MM (34) with 0.3 mM PNP (17) or 0.2 mM 4-NC (14) at 30°C. Media were supplemented with 50 μg ml^{-1} kanamycin or 15 μg ml^{-1} tetracycline when necessary.

Gene knockout, complementation, and expression. The gene knockout and complementation experiments were conducted to identify the physiological role of *pnpG* in PNP degradation *in vivo*. Knockout plasmid pK18*mobsacB*-$_u$*pnpG*$_d$ was constructed by fusing two PCR products to EcoRI/PstI-digested pK18*mobsacB* (35, 36) with the In-Fusion HD cloning kit. These two PCR products were the upstream and downstream fragments of *pnpG* amplified using two pairs of primers, primer pair KO-*pnpG*-uF and KO-*pnpG*-uR and primer pair KO-*pnpG*-dF and KO-*pnpG*-dR, respectively. After pK18*mobsacB*-$_u$*pnpG*$_d$ was transformed into *E. coli* WM3064 (2,6-diaminopimelic acid auxotroph) (37), transconjugation was done between strains SJ98 and WM3064(pK18*mobsacB*-$_u$*pnpG*$_d$) as described previously (35) to obtain mutant strain SJ98Δ*pnpG*. *pnpG* was amplified using primers GC-*pnpG*-F and GC-*pnpG*-R and fused to PstI/KpnI-digested pRK415 (13, 38) to produce the complementation plasmid pRK415-*pnpG*. pRK415-*pnpG* was also transformed into strain SJ98Δ*pnpG* to obtain the complemented strain SJ98Δ*pnpG*(pRK415-*pnpG*) by transconjugation. *pnpA* was amplified using a pair of primers, *pnpA*-F and *pnpA*-R, and inserted into EcoRI-digested pGEX-6P-1, and pGEX-6P-1-*pnpA* was then transformed into *E. coli* BL21(DE3). All the above-described DNA fragments were verified by DNA sequencing to ensure that no mutations had been incorporated during PCR amplification.

Measurement of bacterial growth. The growth of strain SJ98 and its derivatives was measured by the optical density at 600 nm with a Lambda 25 UV-visible (UV-Vis) spectrometer (PerkinElmer, Waltham, MA). The consumption of PNP and 4-NC as well as the accumulation of BQ, HQ, and BT were monitored by high-performance liquid chromatography (HPLC) as previously described (17), with modifications. All the experiments were done in triplicate.

Biotransformation by resting cells. Biotransformation of 4-NC by cells of strain SJ98 and its derivatives was performed as described previously (13), with some modifications. Strain SJ98 and its two variants were grown in MM supplemented with 2 mM glucose and 3 mM $(NH_4)_2SO_4$ to an OD_{600} of 0.3, and 0.2 mM 4-NC was then added for a 6-h induction. Next, cells were separately harvested and washed twice with MM. The cells were then resuspended in MM to an OD_{600} of 2.0. Biotransformation was initiated by adding 0.3 mM 4-NC. Before biotransformation, cells of strains SJ98 and SJ98Δ*pnpG*(pRK415-*pnpG*) were individually preincubated for 10 min with 1 mM 2,2′-dipyridyl, an iron(II) chelator, to inhibit the activity of nonheme Fe(II)-dependent extradiol dioxygenases (39). At appropriate intervals, 0.5-ml samples were withdrawn, mixed with equal volumes of methanol, and shaken vigorously for 5 min to stop the reaction. After centrifugation at 12,000 $\times$ *g* at 4°C for 10 min, the supernatants of samples were used for HPLC analysis. Biotransformation of 4-NC by cells of *E. coli* BL21(DE3)(pGEX-6P-1-*pnpA*), grown on LB with isopropyl-β-D-thiogalactopyranoside (IPTG) induction, was also performed using the above-described method. Quantitative analyses were performed using a standard curve of authentic standards.

TABLE 3 Primers used in this study

Primer	Sequence (5′–3′)	Purpose
KO-*pnpG*-uF	CTATGACATGATTACGAATTCATCGCTGCCC AAAGGTCTTT	Amplification of the upstream fragment of *pnpG* for gene knockout
KO-*pnpG*-uR	CTTCGTCTCTGATGTCCTCACGCGATCGAC	
KO-*pnpG*-dF	TGAGGACATCAGAGACGAAGAGA TGAGCTCTATTAGC	Amplification of the downstream fragment of *pnpG* for gene knockout
KO-*pnpG*-dR	GCCAAGCTTGCATGCCTGCAGCAGT GGATGTTATGGAGGGTCTTT	
GC-*pnpG*-F	GCCAAGCTTGCATGCCTGCAGATGAATACG ACAACTGAGCGCC	Amplification of *pnpG* for gene complementation
GC-*pnpG*-R	AGTGAATTCGAGCTCGGTACCTTAAGCGTTT GCTCGACTGAGC	
SJ98-RTq-*pnpA*-F	CGTCGCAACGAATGTCTTCTATG	Amplification of the 172-bp fragment of *pnpA* for real-time qPCR
SJ98-RTq-*pnpA*-R	CATACGACGACGCACTTCCTC	
SJ98-RTq-*pnpG*-F	GAAGAATGGCGCAAAGGTATTG	Amplification of the 116-bp fragment of *pnpG* for real-time qPCR
SJ98-RTq-*pnpG*-R	TCATCGAGCATGATGGACAAG	
SJ98-RTq-16S-F	CGTGTAGCAGTGAAATGCGTAGAG	Amplification of the 142-bp fragment of 16S rRNA genes for real-time qPCR
SJ98-RTq-16S-R	GACATCGTTTAGGGCGTGGAC	
pnpA-F	CCGCGTGGATCCCCGGAATTCATGGAAA CGCTTGAAGGAGTGG	Amplification of *pnpA* for expression
pnpA-R	CTCGAGTCGACCCGGGAATTCTTACGCTG CAAGCTTAAGAGGC	

High-performance liquid chromatography. HPLC was performed at 30°C with a Waters e2695 separation module with a 2998 PDA detector equipped with a C_{18} reverse-phase column (5 μm, 4.6 by 250 mm; Agilent Technologies). The mobile phase consisted of a linear gradient of solvent A (0.1% acetic acid in water) and solvent B (methanol). Solvent B was increased from 30% to 80% in the first 10 min and then held at 80% from 10 to 15 min. The flow rate was 1.0 ml min^{-1}. The injection volume was 10 μl. The substrates PNP and 4-NC were monitored at 317 nm and 345 nm, respectively, while the products BQ and HQ were both detected at 260 nm, and BT was detected at 289 nm. Under these conditions, the retention times of PNP, 4-NC, BQ, HQ, and BT were 8.9 min, 7.3 min, 5.0 min, 3.5 min, and 2.9 min, respectively.

Real-time quantitative PCR. Strain SJ98 was grown in MM with 2 mM glucose to an OD_{600} of 0.3. Cells were harvested, washed by centrifugation, and then separately incubated with 0.1 mM 4-NC and 0.3 mM PNP for 5 h for induction; cells incubated without 4-NC or PNP were used as a negative control. The total RNA was isolated from strain SJ98 cells by using an RNA prep pure bacterial kit (Sangon Biotech, Shanghai, China) and reverse transcribed into cDNA using a PrimeScript RT reagent kit with gDNA (genomic DNA) Eraser (Perfect real time) (TaKaRa, Dalian, China). Real-time quantitative PCR (RT-qPCR) was performed with a CFX Connect real-time PCR detection system (Bio-Rad, Hercules, CA) using iQ SYBR green supermix (Bio-Rad, Hercules, CA) and three pairs of primers, SJ98-RTq-*pnpA*-F and SJ98-RTq-*pnpA*-R, SJ98-RTq-*pnpG*-F and SJ98-RTq-*pnpG*-R, and SJ98-RTq-16S-F and SJ98-RTq-16S-R. The amount of target mRNA was normalized to that of 16S rRNA with the $2^{-\Delta\Delta CT}$ method (40).

Genome sequencing of strain JS425. Strain JS425 was cultured in 100 ml of LB medium until an OD_{600} of 0.8 was reached, and the cells were washed and harvested prior to genome sequencing. The genome isolated from strain JS425 was sequenced using an Illumina NovaSeq system and a PacBio Sequel system at Shanghai Personal Biotechnology Co. Ltd.

Bioinformatics analysis. Among the protein sequences encoded by 775 completely sequenced bacterial genomes from *Pseudomonas* and *Burkholderia*, those from *Pseudomonas* sp. strain JS425 were sequenced and annotated in this study, and the others were downloaded from the Complete Microbial Genomes Database of the National Center for Biotechnology Information (NCBI) (https://ftp.ncbi.nih.gov/genomes/genbank/bacteria/) in May 2020. All of them were used to build a local BLAST database. BLASTp searches were performed with PnpA, PnpB, PnpC, PnpD, PnpE, PnpF, and PnpG against those annotated proteins from 775 completely sequenced bacterial genomes, and for high accuracy of the alignment, the E value was less than 10^{-5}. The proteins encoded by defined *pnp* genes exhibited ≥40% identities with their counterparts in PnpABCDEFG from strain SJ98.

Data availability. The genome sequence of *Pseudomonas* sp. strain JS425 has been deposited in GenBank under accession numbers CP073661 and CP073662. GenBank accession numbers are given in the text for all mentioned genomes, proteins, and genes. GenBank assembly accession numbers are given in Table S2 in the supplemental material for all 775 genomes.

SUPPLEMENTAL MATERIAL

Supplemental material is available online only.

SUPPLEMENTAL FILE 1, PDF file, 1.1 MB.

ACKNOWLEDGMENTS

This work is supported by the National Key Research and Development Program of China (number 2018YFA0901200), the National Natural Science Foundation of China (number 31670107), and the SJTU JiRLMDS Joint Research Fund (MDS-JF-2020A01).

REFERENCES

1. Chi XQ, Zhang JJ, Zhao S, Zhou NY. 2013. Bioaugmentation with a consortium of bacterial nitrophenol-degraders for remediation of soil contaminated with three nitrophenol isomers. Environ Pollut 172:33–41. https://doi.org/10.1016/j.envpol.2012.08.002.
2. Guo X, Wang Z, Zhou S. 2004. The separation and determination of nitrophenol isomers by high-performance capillary zone electrophoresis. Talanta 64:135–139. https://doi.org/10.1016/j.talanta.2004.01.020.
3. Shen W, Liu W, Zhang J, Tao J, Deng H, Cao H, Cui Z. 2010. Cloning and characterization of a gene cluster involved in the catabolism of *p*-nitrophenol from *Pseudomonas putida* DLL-E4. Bioresour Technol 101:7516–7522. https://doi.org/10.1016/j.biortech.2010.04.052.
4. Wei Q, Liu H, Zhang JJ, Wang SH, Xiao Y, Zhou NY. 2010. Characterization of a *para*-nitrophenol catabolic cluster in *Pseudomonas* sp. strain NyZ402 and construction of an engineered strain capable of simultaneously mineralizing both *para*- and *ortho*-nitrophenols. Biodegradation 21:575–584. https://doi.org/10.1007/s10532-009-9325-4.
5. Zhang JJ, Liu H, Xiao Y, Zhang XE, Zhou NY. 2009. Identification and characterization of catabolic *para*-nitrophenol 4-monooxygenase and *para*-benzoquinone reductase from *Pseudomonas* sp. strain WBC-3. J Bacteriol 191:2703–2710. https://doi.org/10.1128/JB.01566-08.
6. Spain JC, Gibson DT. 1991. Pathway for biodegradation of *p*-nitrophenol in a *Moraxella* sp. Appl Environ Microbiol 57:812–819. https://doi.org/10.1128/AEM.57.3.812-819.1991.
7. Zhang S, Sun W, Xu L, Zheng X, Chu X, Tian J, Wu N, Fan Y. 2012. Identification of the *para*-nitrophenol catabolic pathway, and characterization of three enzymes involved in the hydroquinone pathway, in Pseudomonas sp. 1-7. BMC Microbiol 12:27. https://doi.org/10.1186/1471-2180-12-27.
8. Kadiyala V, Spain JC. 1998. A two-component monooxygenase catalyzes both the hydroxylation of *p*-nitrophenol and the oxidative release of nitrite from 4-nitrocatechol in *Bacillus sphaericus* JS905. Appl Environ Microbiol 64:2479–2484. https://doi.org/10.1128/AEM.64.7.2479-2484.1998.
9. Kitagawa W, Kimura N, Kamagata Y. 2004. A novel *p*-nitrophenol degradation gene cluster from a gram-positive bacterium, *Rhodococcus opacus* SAO101. J Bacteriol 186:4894–4902. https://doi.org/10.1128/JB.186.15.4894-4902.2004.
10. Perry LL, Zylstra GJ. 2007. Cloning of a gene cluster involved in the catabolism of *p*-nitrophenol by *Arthrobacter* sp. strain JS443 and characterization of the *p*-nitrophenol monooxygenase. J Bacteriol 189:7563–7572. https://doi.org/10.1128/JB.01849-06.
11. Jain RK, Dreisbach JH, Spain JC. 1994. Biodegradation of *p*-nitrophenol via 1,2,4-benzenetriol by an *Arthrobacter* sp. Appl Environ Microbiol 60:3030–3032. https://doi.org/10.1128/AEM.60.8.3030-3032.1994.
12. Spain JC, Wyss O, Gibson DT. 1979. Enzymatic oxidation of *p*-nitrophenol. Biochem Biophys Res Commun 88:634–641. https://doi.org/10.1016/0006-291x(79)92095-3.
13. Min J, Zhang JJ, Zhou NY. 2014. The gene cluster for *para*-nitrophenol catabolism is responsible for 2-chloro-4-nitrophenol degradation in *Burkholderia* sp. strain SJ98. Appl Environ Microbiol 80:6212–6222. https://doi.org/10.1128/AEM.02093-14.
14. Vikram S, Pandey J, Kumar S, Raghava GP. 2013. Genes involved in degradation of *para*-nitrophenol are differentially arranged in form of non-contiguous gene clusters in *Burkholderia* sp. strain SJ98. PLoS One 8:e84766. https://doi.org/10.1371/journal.pone.0084766.
15. Vikram S, Pandey J, Bhalla N, Pandey G, Ghosh A, Khan F, Jain RK, Raghava GPS. 2012. Branching of the *p*-nitrophenol (PNP) degradation pathway in *Burkholderia* sp. strain SJ98: evidences from genetic characterization of PNP gene cluster. AMB Express 2:30. https://doi.org/10.1186/2191-0855-2-30.
16. Wei M, Zhang JJ, Liu H, Zhou NY. 2010. *para*-Nitrophenol 4-monooxygenase and hydroxyquinol 1,2-dioxygenase catalyze sequential transformation of 4-nitrocatechol in *Pseudomonas* sp. strain WBC-3. Biodegradation 21:915–921. https://doi.org/10.1007/s10532-010-9351-2.
17. Chauhan A, Pandey G, Sharma NK, Paul D, Pandey J, Jain RK. 2010. *p*-Nitrophenol degradation via 4-nitrocatechol in *Burkholderia* sp. SJ98 and cloning of some of the lower pathway genes. Environ Sci Technol 44:3435–3441. https://doi.org/10.1021/es9024172.
18. Hoffmann D, Iinuma Y, Herrmann H. 2007. Development of a method for fast analysis of phenolic molecular markers in biomass burning particles using high performance liquid chromatography/atmospheric pressure chemical ionisation mass spectrometry. J Chromatogr A 1143:168–175. https://doi.org/10.1016/j.chroma.2007.01.035.
19. Wang X, Gu R, Wang L, Xu W, Zhang Y, Chen B, Li W, Xue L, Chen J, Wang W. 2017. Emissions of fine particulate nitrated phenols from the burning of five common types of biomass. Environ Pollut 230:405–412. https://doi.org/10.1016/j.envpol.2017.06.072.
20. Yu CH, Li Y, Zhao X, Yang SQ, Li L, Cui NX, Rong L, Yi ZC. 2019. Benzene metabolite 1,2,4-benzenetriol changes DNA methylation and histone acetylation of erythroid-specific genes in K562 cells. Arch Toxicol 93:137–147. https://doi.org/10.1007/s00204-018-2333-6.
21. Feinland RS, Iscowitz S, Bil MS. October 1977. Autoxidizable hair dye containing preparations. US patent 4,054,413.
22. Suenaga H, Koyama Y, Miyakoshi M, Miyazaki R, Yano H, Sota M, Ohtsubo Y, Tsuda M, Miyazaki K. 2009. Novel organization of aromatic degradation pathway genes in a microbial community as revealed by metagenomic analysis. ISME J 3:1335–1348. https://doi.org/10.1038/ismej.2009.76.
23. Tinikul R, Chenprakhon P, Maenpuen S, Chaiyen P. 2018. Biotransformation of plant-derived phenolic acids. Biotechnol J 13:e1700632. https://doi.org/10.1002/biot.201700632.
24. Bugg TDH, Ahmad M, Hardiman EM, Rahmanpour R. 2011. Pathways for degradation of lignin in bacteria and fungi. Nat Prod Rep 28:1883–1896. https://doi.org/10.1039/c1np00042j.
25. Sainsbury PD, Hardiman EM, Ahmad M, Otani H, Seghezzi N, Eltis LD, Bugg TDH. 2013. Breaking down lignin to high-value chemicals: the conversion of lignocellulose to vanillin in a gene deletion mutant of *Rhodococcus jostii* RHA1. ACS Chem Biol 8:2151–2156. https://doi.org/10.1021/cb400505a.
26. Spence EM, Scott HT, Dumond L, Calvo-Bado L, di Monaco S, Williamson JJ, Persinoti GF, Squina FM, Bugg TDH. 2020. The hydroxyquinol degradation pathway in *Rhodococcus jostii* RHA1 and *Agrobacterium* species is an alternative pathway for degradation of protocatechuic acid and lignin fragments. Appl Environ Microbiol 86:e01561-20. https://doi.org/10.1128/AEM.01561-20.
27. Li ST, Zhou JM, Wang HY, Chen XQ. 2002. Phenolic acids in plant-soil-microbe system: a review. Pedosphere 12:1–14.
28. Nordin K, Unell M, Jansson JK. 2005. Novel 4-chlorophenol degradation gene cluster and degradation route via hydroxyquinol in *Arthrobacter chlorophenolicus* A6. Appl Environ Microbiol 71:6538–6544. https://doi.org/10.1128/AEM.71.11.6538-6544.2005.
29. Takenaka S, Okugawa S, Kadowaki M, Murakami S, Aoki K. 2003. The metabolic pathway of 4-aminophenol in *Burkholderia* sp. strain AK-5 differs from that of aniline and aniline with C-4 substituents. Appl Environ Microbiol 69:5410–5413. https://doi.org/10.1128/AEM.69.9.5410-5413.2003.
30. Travkin VM, Solyanikova IP, Golovleva LA. 2006. Hydroxyquinol pathway for microbial degradation of halogenated aromatic compounds. J Environ Sci Health B 41:1361–1382. https://doi.org/10.1080/03601230600964159.
31. Schafer A, Harms H, Zehnder AJ. 1996. Biodegradation of 4-nitroanisole by two *Rhodococcus* spp. Biodegradation 7:249–255. https://doi.org/10.1007/BF00058184.

32. Bertani G. 2004. Lysogeny at mid-twentieth century: P1, P2, and other experimental systems. J Bacteriol 186:595–600. https://doi.org/10.1128/jb.186.3.595-600.2004.
33. Bertani G. 1951. Studies on lysogenesis. I. The mode of phage liberation by lysogenic *Escherichia coli*. J Bacteriol 62:293–300. https://doi.org/10.1128/JB.62.3.293-300.1951.
34. Liu H, Zhang JJ, Wang SJ, Zhang XE, Zhou NY. 2005. Plasmid-borne catabolism of methyl parathion and *p*-nitrophenol in *Pseudomonas* sp. strain WBC-3. Biochem Biophys Res Commun 334:1107–1114. https://doi.org/10.1016/j.bbrc.2005.07.006.
35. Deng S-K, Zhang W-M, Wang J-P, Gao Y-Z, Xu Y, Zhou N-Y. 2019. Single point mutation in the transcriptional regulator PnpR renders Pseudomonas sp. strain WBC-3 capable of utilizing 2-chloro-4-nitrophenol. Int Biodeterior Biodegradation 143:104732. https://doi.org/10.1016/j.ibiod.2019.104732.
36. Schäfer A, Tauch A, Jäger W, Kalinowski J, Thierbach G, Pühler A. 1994. Small mobilizable multi-purpose cloning vectors derived from the *Escherichia coli* plasmids pK18 and pK19: selection of defined deletions in the chromosome of *Corynebacterium glutamicum*. Gene 145:69–73. https://doi.org/10.1016/0378-1119(94)90324-7.
37. Metcalf WW, Wolfe RS. 1998. Molecular genetic analysis of phosphite and hypophosphite oxidation by *Pseudomonas stutzeri* WM88. J Bacteriol 180:5547–5558. https://doi.org/10.1128/JB.180.21.5547-5558.1998.
38. de Lorenzo V, Eltis L, Kessler B, Timmis KN. 1993. Analysis of Pseudomonas gene products using *lacI*^{q}/*Ptrp-lac* plasmids and transposons that confer conditional phenotypes. Gene 123:17–24. https://doi.org/10.1016/0378-1119(93)90533-9.
39. Vaillancourt FH, Bolin JT, Eltis LD. 2006. The ins and outs of ring-cleaving dioxygenases. Crit Rev Biochem Mol Biol 41:241–267. https://doi.org/10.1080/10409230600817422.
40. Livak KJ, Schmittgen TD. 2001. Analysis of relative gene expression data using real-time quantitative PCR and the $2^{-\Delta\Delta CT}$ method. Methods 25:402–408. https://doi.org/10.1006/meth.2001.1262.
41. Kumar S, Vikram S, Raghava GPS. 2012. Genome sequence of the nitroaromatic compound-degrading bacterium *Burkholderia* sp. strain SJ98. J Bacteriol 194:3286. https://doi.org/10.1128/JB.00497-12.
42. Hernandez-Mendoza A, Martinez-Ocampo F, Lozano-Aguirre Beltran LF, Popoca-Ursino EC, Ortiz-Hernandez L, Sanchez-Salinas E, Dantan-Gonzalez E. 2014. Draft genome sequence of the organophosphorus compound-degrading *Burkholderia zhejiangensis* strain CEIB S4-3. Genome Announc 2:e01323-14. https://doi.org/10.1128/genomeA.01323-14.
43. Li YY, Zhou B, Li W, Peng X, Zhang JS, Yan YC. 2008. Mineralization of *p*-nitrophenol by a new isolate *Arthrobacter* sp. Y1. J Environ Sci Health B 43:692–697. https://doi.org/10.1080/03601230802388793.
44. Iwaki H, Abe K, Hasegawa Y. 2007. Isolation and characterization of a new 2,4-dinitrophenol-degrading bacterium *Burkholderia* sp. strain KU-46 and its degradation pathway. FEMS Microbiol Lett 274:112–117. https://doi.org/10.1111/j.1574-6968.2007.00816.x.
45. Meulenberg R, Pepi M, de Bont JA. 1996. Degradation of 3-nitrophenol by *Pseudomonas putida* B2 occurs via 1,2,4-benzenetriol. Biodegradation 7:303–311. https://doi.org/10.1007/BF00115744.
46. Pakala SB, Gorla P, Pinjari AB, Krovidi RK, Baru R, Yanamandra M, Merrick M, Siddavattam D. 2007. Biodegradation of methyl parathion and *p*-nitrophenol: evidence for the presence of a *p*-nitrophenol 2-hydroxylase in a Gram-negative *Serratia* sp. strain DS001. Appl Microbiol Biotechnol 73:1452–1462. https://doi.org/10.1007/s00253-006-0595-z.
47. Armstrong S, Patel TR. 1993. 1,3,5-Trihydroxybenzene biodegradation by *Rhodococcus* sp. BPG-8. Can J Microbiol 39:175–179. https://doi.org/10.1139/m93-024.
48. Armstrong S, Patel TR. 1992. Utilization of 1,3,5-trihydroxybenzene (phloroglucinol) by a soil isolate, *Rhodococcus* species BPG-8. J Basic Microbiol 32:3–11. https://doi.org/10.1002/jobm.3620320102.
49. Chapman PJ, Ribbons DW. 1976. Metabolism of resorcinylic compounds by bacteria: orcinol pathway in *Pseudomonas putida*. J Bacteriol 125:975–984. https://doi.org/10.1128/JB.125.3.975-984.1976.
50. Zhong Q, Zhang H, Bai W, Li M, Li B, Qiu X. 2007. Degradation of aromatic compounds and degradative pathway of 4-nitrocatechol by *Ochrobactrum* sp. B2. J Environ Sci Health A Tox Hazard Subst Environ Eng 42:2111–2116. https://doi.org/10.1080/10934520701627108.
51. Min J, Wang J, Chen W, Hu X. 2018. Biodegradation of 2-chloro-4-nitrophenol via a hydroxyquinol pathway by a Gram-negative bacterium, *Cupriavidus* sp. strain CNP-8. AMB Express 8:43. https://doi.org/10.1186/s13568-018-0574-7.
52. Pandey J, Heipieper HJ, Chauhan A, Arora PK, Prakash D, Takeo M, Jain RK. 2011. Reductive dehalogenation mediated initiation of aerobic degradation of 2-chloro-4-nitrophenol (2C4NP) by *Burkholderia* sp. strain SJ98. Appl Microbiol Biotechnol 92:597–607. https://doi.org/10.1007/s00253-011-3254-y.